

Supplementary Information

Investigating the mechanotransduction of transient shear stress mediated by Piezo1 ion channel using a 3D printed dynamic gravity pump

Gianmarco Concilia ^{1,*,†}, Austin Lai ^{2,*,†}, Peter Thurgood ¹, Elena Pirogova ¹,

Sara Baratchi ^{2,**,†}, Khashayar Khoshmanesh ^{1,**,†}

¹ School of Engineering, RMIT University, Melbourne, Victoria, Australia

² School of Health & Biomedical Sciences, RMIT University, Bundoora, Victoria, Australia

† Corresponding authors:

Gianmarco Concilia: gianmarco.concilia@student.rmit.edu.au

Austin Lai: s3382962@student.rmit.edu.au

Sara Baratchi: sara.baratchi@rmit.edu.au

Khashayar Khoshmanesh: khashayar.khoshmanesh@rmit.edu.au

*, **: These authors contributed equally to this work.

Keywords: microfluidics, 3D printing, pump, transient flow

Supplementary Information 1: Conceptual diagram of the dynamic gravity pump

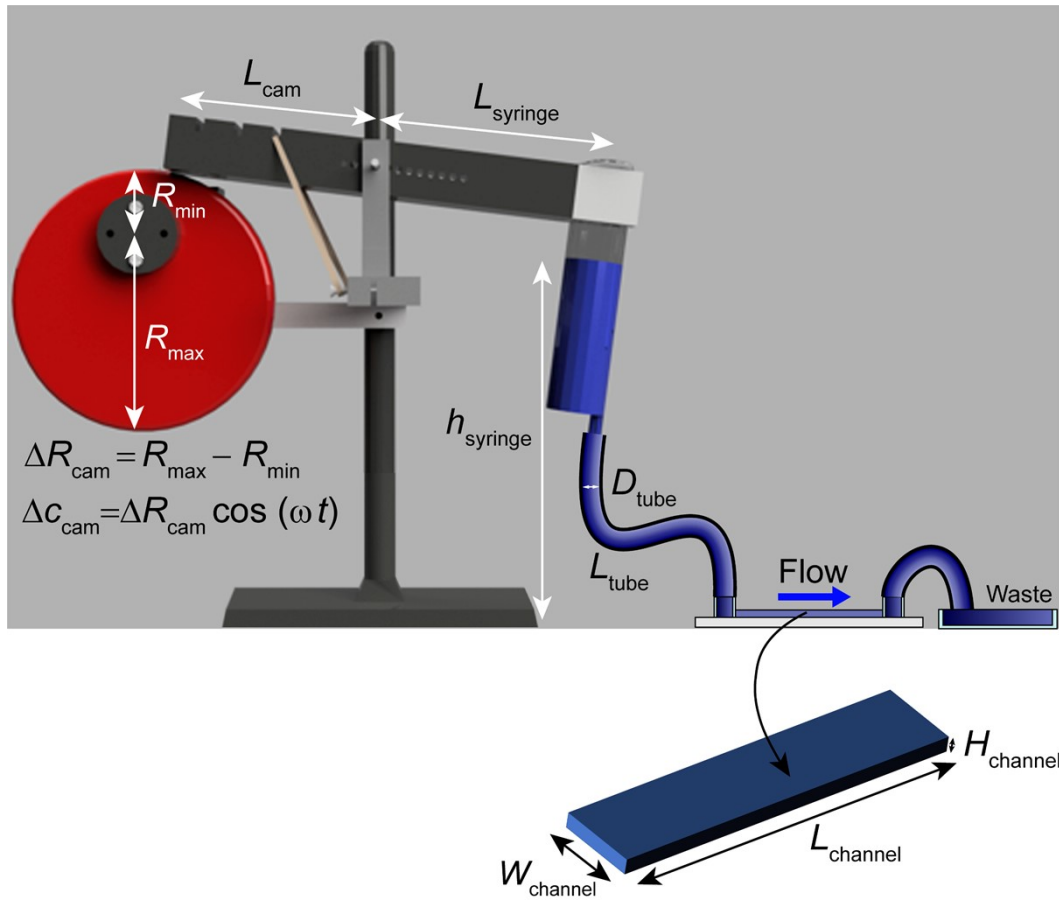


Figure S1. Conceptual diagram of the dynamic gravity pump, illustrating the influential parameter affecting its performance.

Supplementary Information 2: Viscous pressure drop along the tube and microfluidic channel

Given the laminar nature of the flow through the tube, ΔP_{tube} is obtained using the Hagen-Poiseuille equation, as defined below:

$$\Delta P_{tube} = \frac{128 \mu Q(t) L_{tube}}{\pi D_{tube}^4} \quad (S1)$$

in which μ is the fluid viscosity, $Q(t)$ is the flow rate, L_{tube} is the tube length, and D_{tube} is the tube diameter:

Likewise, $\Delta P_{channel}$ is a variant of Hagen-Poiseuille equation for rectangular channels, which is defined, as below:

$$\Delta P_{channel} = \frac{a \mu Q(t) L_{channel}}{W_{channel} H_{channel}^3} \quad (S2)$$

in which, $L_{channel}$ is the channel length, $W_{channel}$ is the channel width, $H_{channel}$ is the channel

height, and a is a coefficient calculated as
$$a = 12 \left[1 - \frac{192 H_{channel}}{\pi^5 W_{channel}} \tanh\left(\frac{\pi W_{channel}}{2 H_{channel}}\right) \right]^{-1}$$

References:

- 1 Fuerstman, M. J., Lai, A., Thurlow, M. E., Shevkoplyas, S. S., Stone, H. A., & Whitesides, G. M., *Lab on a Chip*, 2007, **7**, 1479-1489.
- 2 Wang, Y. I., & Shuler, M. L., *Lab on a Chip*, 2018, **18**, 2563-2574.

Supplementary Information 3: The dynamic flow rate can be modulated by varying the size of the cam

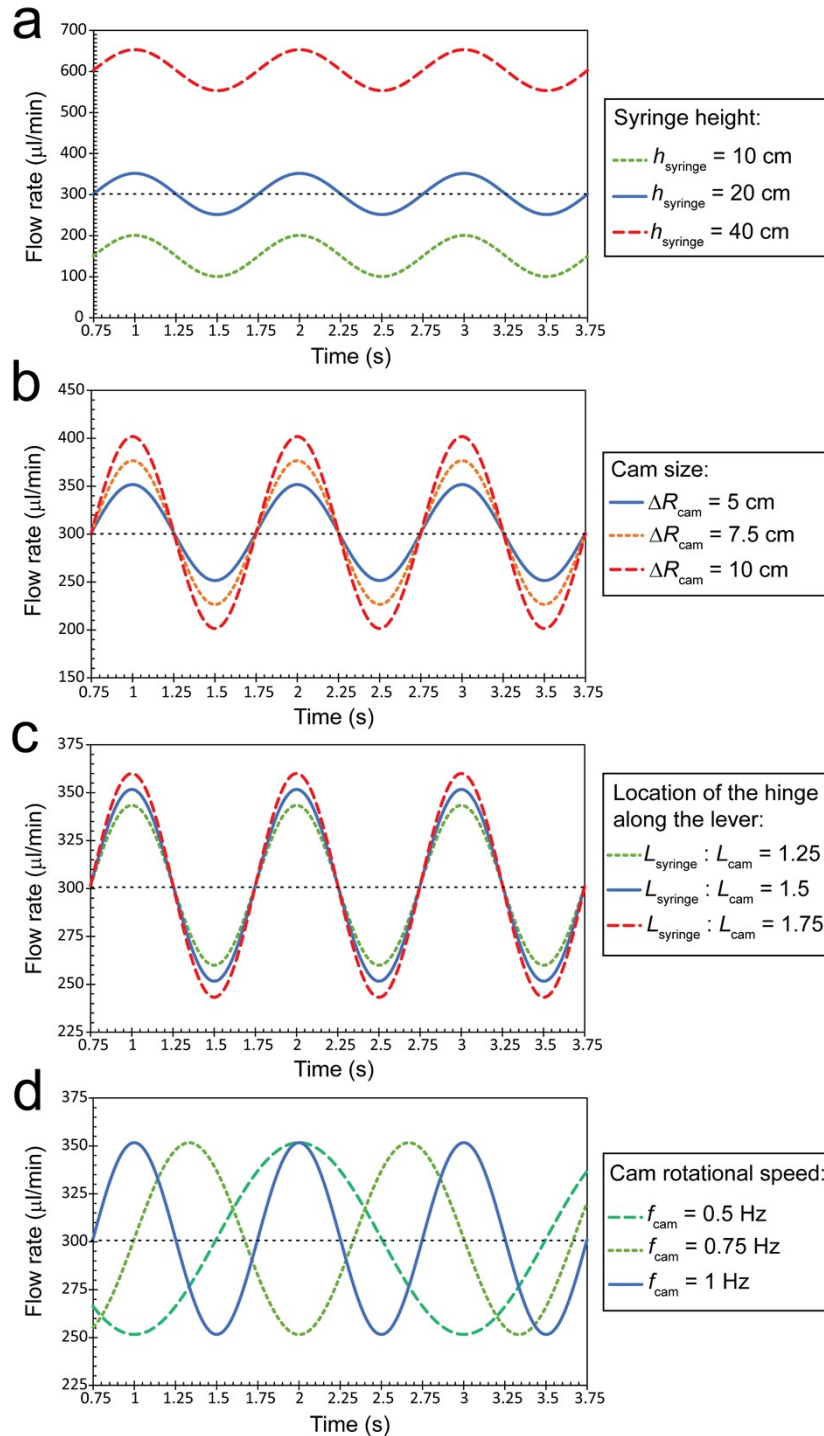


Figure S2. The dynamic flow rate can be modulated by varying the size of the (a) Height of the syringe, (b) Cam size, (c) Location of the hinge along the lever, and (d) Cam rotational speed, as predicted by equation (4).

Supplementary Information 4: Shear stress contours at the floor of the microfluidic channels obtained by numerical simulations

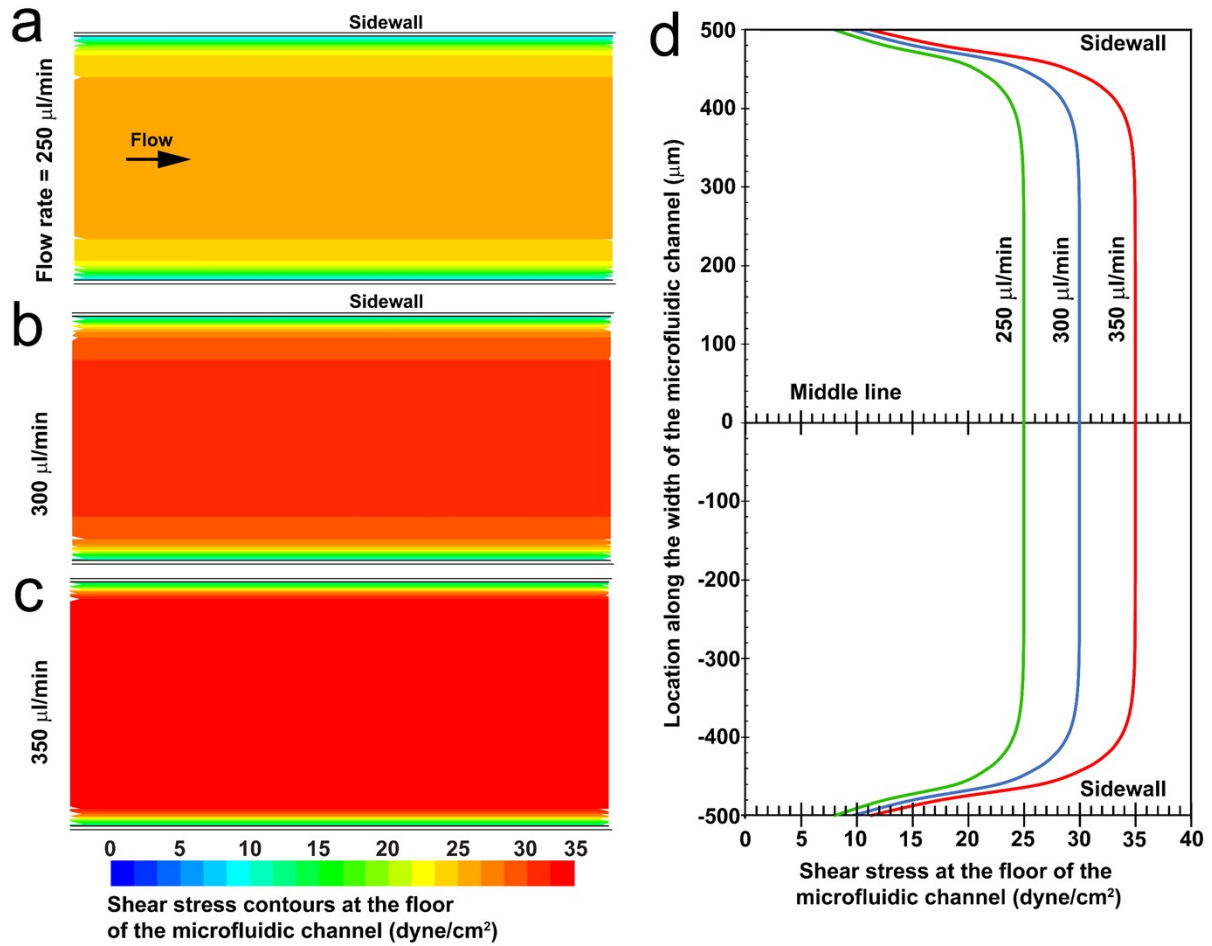


Figure S3. Shear stress contours at the floor of an ibidi μ -slide VI 0.1 microfluidic channel obtained by numerical simulations at various flow rates of (a) 250 $\mu\text{l}/\text{min}$, (b) 300 $\mu\text{l}/\text{min}$, (c) 350 $\mu\text{l}/\text{min}$.

Supplementary Information 5: Geometric specifications of single-sine and double-sine cams

Table S1. Vertical displacement of single-sine and double-sine cams

Single-sine motion:	$\Delta s = 0.5 \times 50 \times \cos(\omega t)$	$0^\circ \leq \omega t \leq 360^\circ$
	$\Delta s_1 = 0.5 \times 50 \times \cos(\omega t)$	$0^\circ \leq \omega t \leq 170^\circ$
	$\Delta s_2 = 0$	$170^\circ \leq \omega t \leq 190^\circ$
Double-sine motion:	$\Delta s_3 = 0.5 \times 32.5 \times \cos(\omega t)$	$190^\circ \leq \omega t \leq 265^\circ$ $285^\circ \leq \omega t \leq 360^\circ$
	$\Delta s_4 = 0$	$265^\circ \leq \omega t \leq 285^\circ$

Supplementary Information 6: Assembly process of the dynamic gravity pump

The pump has 13 major components (**Figure 1a-b**), as briefly described here: (1) The cam connector holds the cam onto the stepper motor. (2) The cam spins to raise and lower the lever based on its variable shape. (3) The rubber band serves as a counterweight and holds down the lever onto the cam ensuring it follows the path of the cam. (4) The lever changes its height based on the movement of the cam raising and lowering the syringe. (5) The lever holder uses the variable holes on the lever attachment to align the lever onto the cam at the desired height change. (6) The support stand holds the entire pump in place and vertically aligns the other components. (7) The syringe holder sits at the end of the lever arm and holds the syringe; it can be interchanged for different syringe sizes. (8) The syringe contains the liquid, and its movement changes the flow rate based on the principles of the gravity pump. (9) The Tygon® tubing connects the syringe to a microfluidic channel. (10) The microfluidic channel is cultured with cells that are subjected to the flow-induced shear stress. (11) The SLI-1000 liquid flow meter (Sensirion) monitors the flow rate of the liquid driven through the microfluidic channel. (12) Stepper motor spins the cam at desired speeds. (13) The motor holder holds the stepper motor on place in the stand.

The design is assembled by putting the stepper motor onto the holder then slotting it through the motor and lever holder. Next, the cam and the holder are put onto the motor and secured. This is followed by placing the lever into place with a 3D printed shaft and attaching the rubber band at the end of the holder and on top of the lever arm. Various components of the pump need to be bolted carefully to avoid undesired vibrations. Lastly, the syringe is added onto the syringe holder and interfaced with the microfluidic channel using a Tygon® tube. The tube was tied to the table using tape to minimise its vibrations and avoiding the tube hitting the table, producing noise in the flow sensor. The microfluidic channel and the liquid flow meter are then interconnected using a secondary Tygon® tube. The design takes around 2.7 hours to print and around 1 hour to assemble.

Supplementary Information 7: The cam-driven dynamic gravity pump can be placed next to a confocal microscope

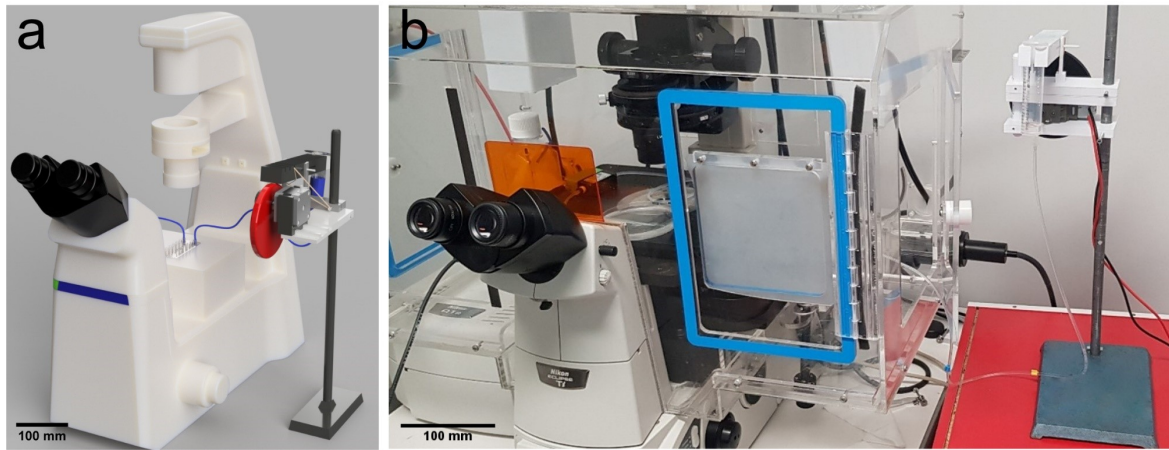


Figure S4. The cam-driven dynamic gravity pump can be placed next to a confocal microscope during calcium signalling experiments: (a) Schematics. (b) Real photograph showing the dynamic gravity pump next to a Nikon confocal microscope.

Supplementary Information 8: Calcium activity of Piezo1-mCherry-HEK293T cells

Table S2. Investigating the effect of transient shear stress on the calcium activity of Piezo1-mCherry-HEK293T cells, presented in Figure 4

	20 dyne/cm ²		60 dyne/cm ²	
	Constant	Transient	Constant	Transient
Peak response	1.4 ± 0.05	1.2 ± 0.03	2.4 ± 0.08	1.7 ± 0.09
Response time	36.9 ± 1.4 s	34.0 ± 4.0 s	21.1 ± 0.2 s	20.0 ± 0.3 s
Activation duration	22.0 ± 2.1 s	14.7 ± 2.6 s	35.4 ± 3.5 s	12.0 ± 0.7 s

Table S3. Investigating the effect of substrate coating on the calcium activity of Piezo1-mCherry-HEK293T cells, presented in Figure 5

	Coating	20 dyne/cm ²		60 dyne/cm ²	
		Constant	Transient	Constant	Transient
Peak response	Poly-L-lysine	1.4 ± 0.05	1.2 ± 0.03	2.4 ± 0.08	1.7 ± 0.09
	Fibronectin	2.0 ± 0.05	2.1 ± 0.08	2.7 ± 0.08	2.6 ± 0.10
Response time	Poly-L-lysine	36.9 ± 1.4 s	34.0 ± 4.0 s	21.1 ± 0.2 s	20.0 ± 0.3 s
	Fibronectin	27.3 ± 0.6 s	29.4 ± 0.7 s	19.8 ± 0.2 s	21.9 ± 0.2 s
Activation duration	Poly-L-lysine	22.0 ± 2.1 s	14.7 ± 2.6 s	35.4 ± 3.5 s	12.0 ± 0.7 s
	Fibronectin	47.4 ± 4.0 s	56.2 ± 3.7 s	30.2 ± 2.7 s	44.1 ± 4.0 s